McWhirter Graduate Research Symposium

Friday, September 20th, 2019

HUB Robeson Center

8:45 AM	**Registration (129B)**				
9:20 AM	**Session 1**	**Room 129 A**		**Room 129C**	
		From ^{13}C labeling data to a core metabolism kinetic model: A kinetic model parameterization pipeline	Charles Foster	*Predicting an Optimal Oxide/Metal Interface Catalyst for Hydrodeoxygenation Chemistry of Biomass Derivatives*	Shyam Deo
		Enzyme-coated liposomes as dual-direction self-propulsive motors	Ambika Somasundar	*Searching for correlations between IR and Raman spectral features and bond length and angle distributions of silicate glass network*	Hongshen Liu
		Simultaneous regulation of many genes using CRISPRi and highly non-repetitive extra long sgRNA arrays (ELSAs)	Alexander Reis	*Entanglement in semiflexible polymer melts and solutions from simulations*	Vineeth Bobbili
		High Mobility and Drive Current ZnO Thin Film Transistors	Sang H. Yoo	*Role of Chloride in the Shape-Selective Growth of Copper Nanocrystals*	Zihao Chen
10:40 -11	**COFFEE BREAK**				
		Process Development of a Precipitation-Filtration Unit for Recombinant Protein Capture	Zhao Li	*Heterometallic hierarchical MOFs from intergrowth and their increased selectivity in light hydrocarbon/methane separation*	Xinyang Yin
		Influence of Doping on the performance of Solid Polymer Electrolyte for Lithium–ion batteries	Shankar Ram	*Plasma-Driven Catalysis for SO_2 Reduction to Elemental Sulfur*	Mohammad S Alqahtani
		Grazing Incidence X-ray Scattering Reveals Cellulose Texture in Primary Plant Cell Walls	Sintu Rongpipi	*Hydrothermal Valorization of Food Waste*	Bita Motavaf

12 PM	**Lunch (Room 232 A/B)**		
1 PM	**Keynote speaker (Dr.Susan Fullerton) Room 129 AB**		
2 PM	**Session 2**	**Room 129C**	
		High-Performance Multi-Component Organic Solar Cells	Alperen Ayhan
		DFT analysis of Amino Acid functionalization of Hematite for electroreduction catalysis	Sharad Maheshwari
		Morphing simulations reveal architecture effects on polymer miscibility in bead spring chains	Shreya Shetty
		Metal-Organic Framework (MOF) assisted Li^+ conduction in solid polymer electrolyte for application in lithium-ion batteries	Nagma Zerin
		Probing Nanocrystal Shape Transformations Using Replica-exchange Molecular Dynamics	Tianyu Yan
		Morphology and transport properties of ion-exchange membranes for applications in advanced flow batteries	Nayan Saikia
4:00 PM	**POSTER SESSION 129 AB**		

From ^{13}C labeling data to a core metabolism kinetic model: A kinetic model parameterization pipeline

Presenter: Charles Foster (cjf33@psu.edu)
Advisor: Costas Maranas (cdm8@psu.edu)

Kinetic models of metabolic networks offer the promise of quantitative phenotype prediction. The mechanistic characterization of enzyme catalyzed reactions allows for tracing the effect of perturbations in metabolite concentrations and reaction fluxes in response to genetic and environmental perturbation that are beyond the scope of stoichiometric models. In this study, we develop a two-step computational pipeline for the rapid parameterization of kinetic models of metabolic networks using a curated metabolic model and available ^{13}C-labeling distributions under multiple genetic and environmental perturbations. The first step involves the elucidation of all intracellular fluxes in a core model of *E. coli* containing 74 reactions and 61 metabolites using ^{13}C-Metabolic Flux Analysis (^{13}C-MFA). Here, fluxes corresponding to the mid-exponential growth phase are elucidated for seven single gene deletion mutants from upper glycolysis, pentose phosphate pathway and the Entner-Doudoroff pathway. The computed flux ranges are then used to parameterize the same (i.e., k-ecoli74) core kinetic model for *E. coli* with 55 substrate-level regulations using the newly developed K-FIT parameterization algorithm. The K-FIT algorithm employs a combination of equation decomposition and iterative solution techniques to evaluate steady-state fluxes in response to genetic perturbations. k-ecoli74 predicted 86% of flux values for strains used during fitting within a single standard deviation of ^{13}C-MFA estimated values. By performing both tasks using the same network, errors associated with lack of congruity between the two networks are avoided, allowing for seamless integration of data with model building. Product yield predictions and comparison with previously developed kinetic models indicate shifts in flux ranges and the presence or absence of mutant strains delivering flux towards pathways of interest from training data significantly impact predictive capabilities. Using this workflow, the impact of completeness of fluxomic datasets and the importance of specific genetic perturbations on uncertainties in kinetic parameter estimation are evaluated. In addition to *E. coli* core metabolism, the workflow developed in this study *Clostridium thermocellum* (*C. therm*) core metabolic network (108 reactions, 80 metabolites). ^{13}C-MFA on the core metabolism of wild-type *C. therm* revealed the pyruvate as a previously unidentified source of serine in the core metabolism. A method for systematically identifying likely substrate-level activation and inhibition mechanisms during kinetic parameterization was developed and applied, as enzyme regulatory mechanisms in non-model *C. therm* are largely absent from literature.

Predicting an Optimal Oxide/Metal Interface Catalyst for Hydrodeoxygenation Chemistry of Biomass Derivatives

Presenter: Shyam Deo (sxd375@psu.edu)
Advisor: Michael J. Janik (mjanik@psu.edu)

Selective C-O cleavage is the most difficult chemical transformation en route to fuels production from biomass derivatives such as furfuryl alcohol. Metal oxide-metal interfaces have recently been used to manipulate catalytic selectivity in such multistep reactions, and hinder non-selective decarbonylation (DCO, C-C activation) or aromatic ring hydrogenation. Palladium nanoparticles encapsulated by porous TiO_2 shows high selectivity and activity towards hydrodeoxygenation (HDO) and minimal DCO [1]. Our interfacial model of TiO_2/Pd core-shell catalyst in the form of rutile TiO_2 (110) nanowire over Pd (111) provides qualitative mechanistic determination of the role of interfacial active sites towards deoxygenation and decarbonylation. A much-lowered barrier to HDO is obtained over TiO_{2-x}/Pd oxygen deficient interface model relative to supported Pd catalysts (0.20 eV barrier vs 0.95 eV on Pd (111))[2].

The farther objective is, however, to predict an optimal combination of oxides and metal catalyst with interfacial properties to match the combined hydrogenation and redox requirements of HDO. The search relies on optimising different descriptors that influence the synergy between the oxide and metals' functionalities for the studied reaction. Since oxygen vacancies at the interface activate the C-O bond of the hydroxylated reactants with the alcohol group filling the vacancies in a reverse Mars-van Krevelen mechanism, the HDO activity is correlated with the reducibility of the oxide. The choice of the oxide/metal interface is also governed by tweaking the metal oxide and the metal properties in terms of descriptors like metal–oxygen bond strength, metal-carbon binding energy, metal's work function or its relative gap with the d-band centre. Furthermore, the interface should be equally capable of activating hydrogen to provide a hydrogen environment and complete the final hydrogenation. Herein, we use density functional theory (DFT) to study the elementary surface reactions of furfuryl alcohol over the oxide/metal interface model comprised of metals with varying carbon adsorption energies and oxides' nanowire with varying reducibilities (or tuned by dopants). The mechanistic study is also extended to predict deoxygenation of other stringent oxygenates like m-cresol, phenols etc. with the inclusion of descriptors that account for structural differences and differing C-O bond enthalpies of these oxygenated species. This intends to establish more generic correlations aimed to optimise the overall HDO chemistry, hydrogen activation and subsequent hydrogenation of different oxygenated biomass.

[1] J. Zhang, B. Wang, E. Nikolla, J.W. Medlin, Directing Reaction Pathways through Controlled Reactant Binding at Pd–TiO2 Interfaces, Angewandte Chemie, 129 (2017) 6694-6698.

[2] S. Deo, W. Medlin, E. Nikolla, M.J. Janik, Reaction paths for hydrodeoxygenation of furfuryl alcohol at TiO2/Pd interfaces, Journal of Catalysis, 377 (2019) 28-40.

Enzyme-coated liposomes as dual-direction self-propulsive motors

Presenter: Ambika Somasundar (azs351@psu.edu)
Advisor: Ayusman Sen (asen@psu.edu) & Darrell Velegol (dxv9@psu.edu)

Directional migration in response to specific chemical signals is critical for the survival of living organisms. This enables living cells to move towards food, escape away from toxins, transport cargo and coordinate collective behavior. Model protocells derived from phospholipids and other amphiphiles have been studied and their movement through catalysis has been observed. However, control of directionality based on chemical cues (chemotaxis) has been difficult to achieve. In this talk, I will discuss both positive and negative chemotaxis of autonomous liposomal protocells based on the interplay between enzyme catalysis- induced positive chemotaxis and solute-phospholipid interaction-based negative chemotaxis. In doing so, I will systematically rule out currently available mechanisms of colloidal transport and propose a potentially new and previously unrecognized mechanism of transport due to Hofmeister effect. This opens up the possibility of other mechanisms for the transport of biological colloids. Additionally, controlling the extent and direction of chemotaxis holds considerable potential for designing cell mimics and delivery vehicles that can reconfigure their motion in response to environmental conditions.

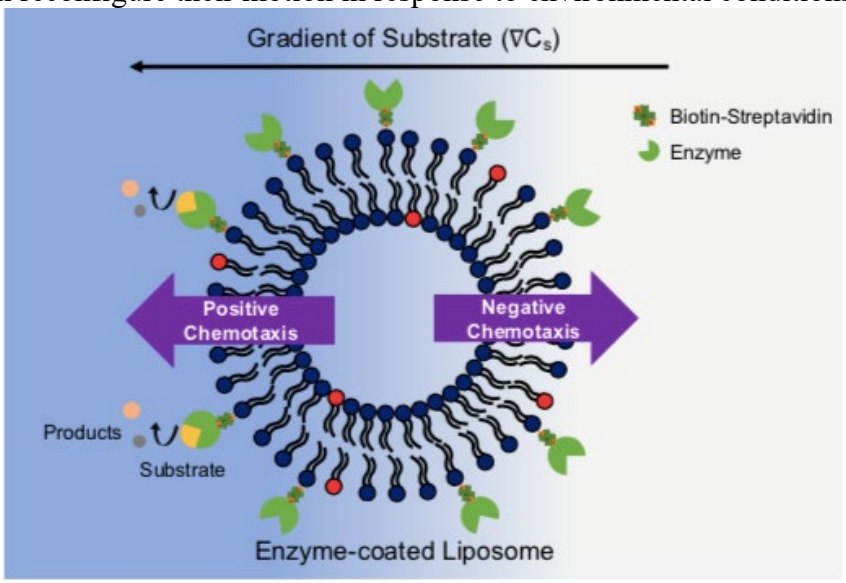

Searching for correlations between IR and Raman spectral features and bond length and angle distributions of silicate glass network

Presenter: Hongshen Liu (hul64@psu.edu)
Advisor: Seong H. Kim (shk10@psu.edu)

Vibrational spectroscopies like infrared (IR) and Raman are useful tools for probing glass structure. However, the vibrational band features in IR and Raman spectra are not fully understood. IR and Raman were performed for a series of sodium silicate glasses; and interpretation in correlation with bond parameters was carried out with assistance of MD simulation reactive force field (ReaxFF) potential. In experimentally measured reflectance IR spectra, as sodium concentration increases, stretching vibrational bands in IR shifts to lower frequency region with intensity decreasing. With MD simulation, it was found that bond length of both Si-BO and Si-NBO get longer as more sodium ions are involved in silicate network. The increase of bond length can be correlated with red shift of stretching vibration Si-O-Si in IR spectra.

Meanwhile, stretching vibrational band in high frequency of Raman spectra shows blue shift with intensity increasing as sodium content increases. In low frequency, bending vibrational band shifts to higher frequency with various peak intensity changing. In Raman spectra, the bands at high frequency and low frequency were assigned to Q^n species and various members of ring respectively. However, our MD simulation showed inconsistent result with previous assignments. It raises question that if Q^n species and ring size assignment in previous work are reasonable.

Simultaneous regulation of many genes using CRISPRi and highly non-repetitive extra long sgRNA arrays (ELSAs)

Presenter: Alexander C. Reis (alex.reis@psu.edu)
Advisor: Howard M. Salis (salis@psu.edu)

Microbial engineering often requires the regulation of many gene expression levels, for example, to redirect metabolic flows or create complex phenotypes. While CRISPR-based systems enable cross-species gene regulation, it remains difficult to express many single-guide RNAs within the same organism without triggering genetic instability, due to the presence of repetitive DNA sequences. Here we stably co-expressed up to 22 single-guide RNAs within highly compact extra-long sgRNA arrays (ELSAs) to simultaneously knock down the expression of many targeted genes by up to 3500-fold. To do this, we developed toolboxes of highly non-repetitive genetic parts, including non-repetitive sgRNA handles, by combining biophysical modeling, biochemical characterization, and machine learning to identify sequence-function relationships. We then developed an automated algorithm to design ELSAs that regulate desired sets of genes, utilizing the developed toolboxes of non-repetitive genetic parts and 23 design rules quantifying DNA synthesis complexity, sgRNA expression levels, sgRNA target selection, and genetic stability. As demonstrations, we introduced designed ELSAs into the *E. coli* genome to create and stably maintain highly selective phenotypes, characterized by long-term growth, RT-qPCR, RNA-Seq, and LC-MS measurements. A 15-sgRNA ELSA targeting *hisD, proC, lysA, tyrA, aroF, pheA, leuA, ilvD,* and *argH* resulted in multiple amino acid auxotrophy. A 20-sgRNA ELSA targeting *poxB, sdhC, sdhD, ackA, pta,* and *iclR* increased succinic acid production by 150-fold. A 22-sgRNA ELSA targeting *yncG, plsB, dkgA, yncE, ansP, narQ, yncH, adiA, iclR, ycfS, marR,* and *wzb* disrupted stress response, inhibited membrane biosynthesis, and reduced persister cell formation by up to 21-fold following antibiotic treatment. Altogether, we show that ELSAs enable simultaneous regulation of many genes for diverse metabolic engineering and synthetic biology applications.

Entanglement in semiflexible polymer melts and solutions from simulations

Presenter: Sai Vineeth Bobbili (szb229@psu.edu)
Advisor: Scott T. Milner (stm9@psu.edu)

Viscoelastic properties of high molecular weight polymer liquids are governed by topological interactions between molecules. Entanglements in polymer melts and solutions arise from constraints imposed by uncrossability of the chains. Multiple scaling arguments have been proposed to describe how the entanglement molecular weight depends on polymer architecture and concentration. The Lin-Noolandi scaling argument, well supported by data for real polymers, assumes that polymers are flexible within their tubes; it fails at some point as chains become stiffer. Everaers has made a different scaling proposal, which crosses over from semiflexible chains to stiff chains as described by Morse. This argument is consistent with simulation data for a range of bead-spring melts, but is not consistent with LN.

We use simulations to explore a wide range of entangled bead-spring ring chains, to find out how entanglement properties vary with chain stiffness and concentration. To vary the packing length over a wider range, we add side groups to make chains bulkier. We calculate entanglement properties using three techniques: chain shrinking to find the primitive path, measuring the tube diameter by the width of the “cloud" of monomer positions about the primitive path, and directly measuring the plateau modulus. As chain stiffness and bulkiness vary, we observe three distinct scaling regimes, consistent with LN scaling, semiflexible chains, and stiff chains.

Influence of Doping on the performance of Solid Polymer Electrolyte for Lithium–ion batteries

Presenter: Shankar C. V. Ram (sxc659@psu.edu)
Advisor: Janna Maranas (jmaranas@psu.edu)

Polyethylene oxide (PEO) based solid polymer electrolytes (SPEs) are an attractive alternative to the flammable liquid/gel electrolytes currently used in rechargeable lithium ion batteries. In addition to improving safety, SPEs could allow the use of Lithium metal anode (3860 mAh/g) which has higher specific energy than commercially used lithium graphite anode (372 mAh/g). This increase in specific energy would greatly improve the range that an electric car can travel before recharging. However, SPEs suffer from low Li^+ ion conductivity. In an amorphous polymer, the conductivity is linked to PEO segmental motion; In order to increase the segmental motion, we must reduce the glass transition temperature (*Tg*). Unfortunately, this increase in polymer dynamics reduces the mechanical strength of SPE. PEO_6-$LiClO_4$ (PEO_6) complex is a tunnel-like PEO/salt co-crystal [Figure] which conducts Li^+ based on a mechanism that decouples conductivity and segmental motion of the polymer. The studies conducted on PEO_6 used very low molecular weight PEO. At this molecular weight, the polymer has very low mechanical stability. In SPEs with high molecular weight PEO, conduction through PEO_6 is unfavorable as the tunnels fold to form lamellar structures and increase the conduction pathway. Our group has used cellulose Nano whiskers to stabilize the PEO_6 structure for ultra-high molecular weight PEO. In spite of the stabilization, conductivity (~10^{-6} S/cm) is still below what is required for practical application.

Inspired from ceramics, we dope PEO_6 with small amounts of anions or cations to increase the conductivity of the SPE. We vary the size of the anion, and cation to create defects in the PEO_6 crystal lattice. We observe up to an order of magnitude increase in the conductivity of doped samples compared to the undoped ones. Interestingly, the increase in conductivity is not correlated with the decrease in Tg of the SPEs [Figure]. We further investigate the influence of doping on the crystalline structure and polymer dynamic using X-Ray (Wide-angle X-ray scattering) and neutron scattering (QENS) techniques.

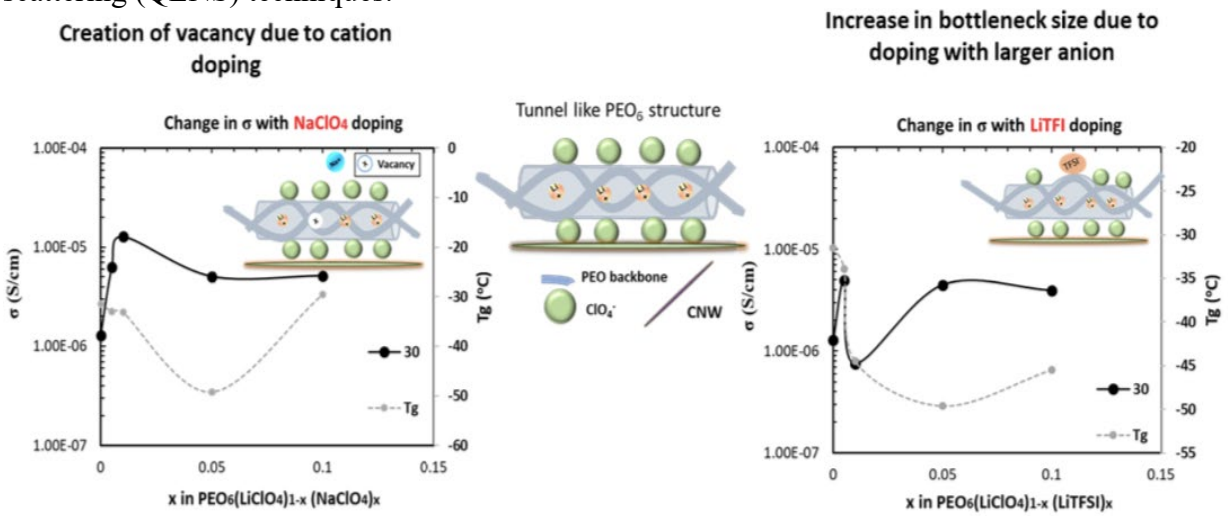

Role of Chloride in the Shape-Selective Growth of Copper Nanocrystals

Presenter: Zihao Chen (zuc12@psu.edu)
Advisor: Kristen Fichthorn (kaf2@psu.edu)

Cu nanocrystals have promising applications in many cutting-edge technologies, which are highly dependent on their morphologies. These nanomaterials are typically synthesized using solution-phase methods, which involve a cupric salt, a capping agent hexadecylamine (HDA), and glucose as the reducing agent. Additionally, chloride is usually introduced as an additive to achieve robust shape control. In the interest of achieving morphology-controlled syntheses, understanding the mechanistic origins of shape selectivity is necessary, but elusive.

It has been proposed that the preferential binding of the capping agent HDA to Cu(100) instead of Cu(111) leads to shape-selective growth, but there is no direct experimental evidence to support this hypothesis. In addition, first-principle calculations based on density functional theory (DFT) show that HDA alone is unlikely to promote the growth of nanowires and nanocubes. Electrochemical experiments indicate that the amount of Cl^- added can serve as a trigger to produce a variety of nanocrystal shapes. Here, we use dispersion-corrected DFT to investigate the possibility that there is a synergy in the binding of HDA and chloride to Cu surfaces, through which different shapes including wires, truncated cubes, and truncated octahedra emerge.

The co-adsorption of HDA and Cl to Cu(100) and Cu(111) is studied. We find that both Cu(100) and Cu(111) are passivated by a dense HDA adlayer at low concentrations of Cl, while repulsive electrostatic interactions between adsorbed Cl and HDA lead to the disruption of the HDA layer at higher concentrations of Cl. An *ab initio* thermodynamics study of various Cu-Cl-HDA surfaces confirms the emergence of truncated octahedra and cubes at these two conditions, respectively. Desorption of the HDA layer occurs at a lower Cl potential/coverage on Cu(111) than on Cu(100). Thus, free Cu atoms can add to the open {111} facets relatively easily compared to well protected {100} facets, leading to the anisotropic growth of Cu nanowires. The shapes predicted are in well agreement with synthetic results, as well as electrochemical results from single crystals of Cu.

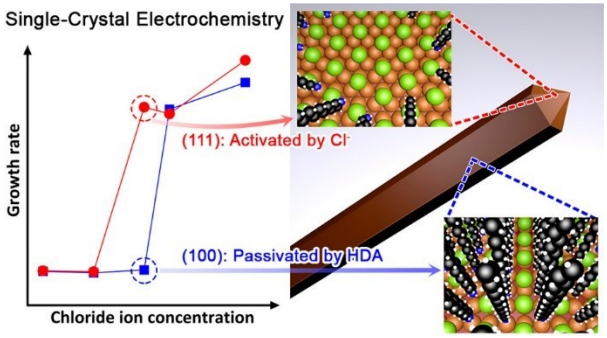

Grazing Incidence X-ray Scattering Reveals Cellulose Texture in Primary Plant Cell Walls

Presenter: Sintu Rongpipi (sxr95@psu.edu)
Advisor: Enrique D. Gomez (edg12@psu.edu) & Esther W. Gomez (ewg10@psu.edu)

Primary plant cell wall is a complex, heterogeneous mixture of several polysaccharides including cellulose, hemicellulose and pectin. Within these cell walls, cellulose exists as microfibrils forming a semi-crystalline structure which plays an important role in regulating biological processes of plant growth and conversion of cellulosic biomass into a renewable energy source. Commercially, cellulose is also an important raw material for paper, textile and construction materials. However, several aspects of crystalline structure of cellulose remain elusive. One such structural parameter is the orientation of cellulose crystallites within the fibrils. This parameter may be an important determinant of the mechanical properties of cell wall as well as cellulose-cellulose and cellulose-matrix interactions.

We studied the structure of cellulose in primary cell walls of plants through grazing incidence wide angle X-ray scattering (GIWAXS), which is a morphological characterization approach that can probe the sample surface as well as beneath it by tuning the angle of incidence. The grazing incidence geometry yields a high signal-to-noise ratio and causes lesser radiation damage, making it ideal for plant cell wall samples which are fragile and weakly scattering. We found that scattering from cellulose and epicuticular wax crystals can be decoupled. Furthermore, treatment of cell walls with cell wall digesting enzymes and chloroform revealed strong texturing of cellulose. The degree of preferred orientation of the crystals was determined through pole figures constructed from the combination of GIWAXS and X-ray Diffraction (XRD) rocking scans. It was found that cellulose texturing depends on the developmental age of the plant tissue and on its source. Furthermore, we found that cellulose texture is disrupted in pectin and cellulose mutants but not in xyloglucan mutants. These findings not only provide fundamental knowledge about the role of cellulose in plant growth and development, but also provide key information about cellulose crystalline structure which can help design cellulose-like materials and efficient biomass conversion processes.

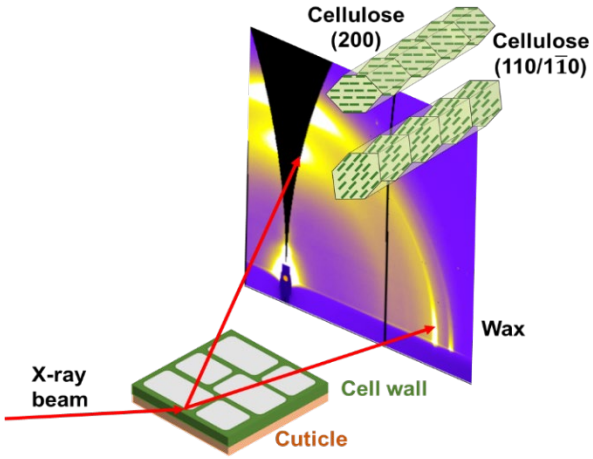

Heterometallic hierarchical MOFs from intergrowth and their increased selectivity in light hydrocarbon/methane separation

Presenter: Xinyang Yin (xuy42@psu.edu)
Advisor: Xueyi Zhang (xuz32@gmail.com)

In this work, we demonstrate heterometallic hierarchical MOF nanoparticles formed by intergrowth of pillared MOFs. Pillared MOF $M^{I}_2(ndc)_2(dabco)$ (M^{I}=Co, Ni, Cu, Zn, ndc=naphthelenedicarboxylic acid, dabco=1,4- diazabicyclo[2.2.2]octane) nanoparticles were synthesized with various morphologies, on which $M^{II}_2(ndc)_2(dabco)$ (M^{II}=Co, Ni, Cu, Zn) nanoparticles were intergrown. Several parameters related to the system were exploited to give a general strategy of intergrowth of MOF nanoparticles, based on which all 12 pairs of bimetallic heteroepitaxial growths among Co, Ni, Cu and Zn were achieved. The intergrown particles preserved the structure, crystallinity, and morphology of their respective primary particles. Adsorption of hydrocarbons (CH_4, ethane, ethene, propane, and propene) at pressures up to 10 bar (absolute) was performed on the MOFs. The hierarchical MOFs have shown increased adsorption of hydrocarbons at low pressures, and IAST selectivity of propane/methane as high as 53 were observed (total pressure 1 bar, CH_4 mole fraction: 0.8), suggesting the hierarchical materials can be used for adsorptive removal of natural gas liquids from crude natural gas.

Process Development of a Precipitation-Filtration Unit for Recombinant Protein Capture

Presenter: Zhao Li (zzl5215@psu.edu)
Advisor: Andrew Zydney (alz3@psu.edu)

Precipitation can be a highly effective capture step in the production of high titer recombinant protein products like monoclonal antibodies. In this work, precipitates with high precipitation yield and consistent morphologies were produced continuously in tubular precipitators using a combination of $ZnCl_2$ and PEG as cross-linking and volume exclusion agents, respectively. Microfiltration was then integrated as part of a continuous operation to concentrate and wash the precipitate slurry to remove non-precipitated impurities, such as host cell proteins (HCP) and DNA, as shown schematically in Figure 1. High degrees of HCP/DNA removal were achieved using multiple tangential flow filtration (TFF) hollow fiber modules in a counter-current configuration, with long term stable operation achieved by operating the membrane modules below the critical filtrate flux for fouling.

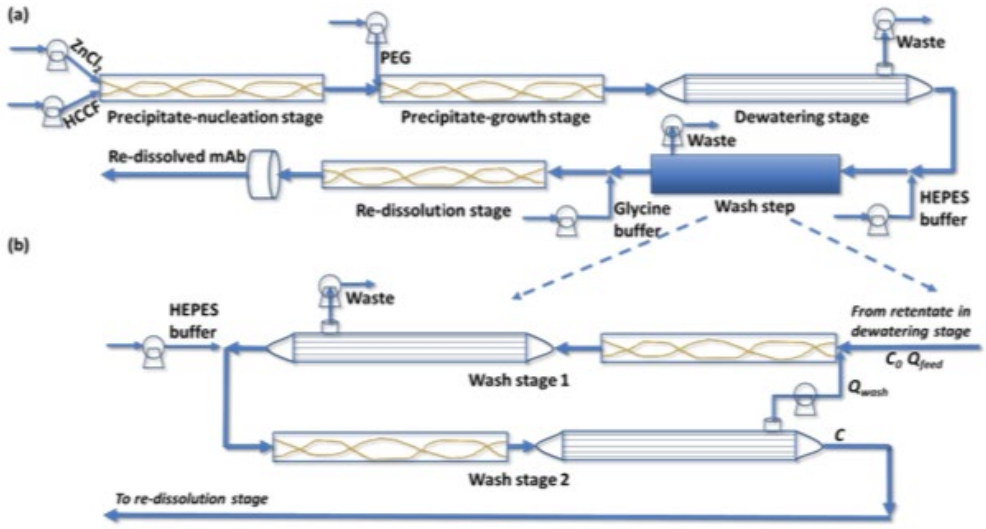

Figure 1 Schematic diagram of the proposed continuous precipitation and filtration method.

Plasma-Driven Catalysis for SO_2 Reduction to Elemental Sulfur

Presenter: Mohammad S. AlQahtani (msa53@psu.edu)
Advisor: Chunshan Song (cxs23@psu.edu)

Plasma-assisted or driven catalysis refers to the combination of gaseous discharge (plasma) and heterogonous catalysis. This coupling can produce outcomes that are not possible by plasma or catalysis separately.

The low temperature conversion of SO_2 to elemental sulfur in a single catalytic step remains elusive. In this study, we report a novel low temperature one-step plasma-driven catalytic process for direct SO_2 reduction to elemental sulfur in DBD packed bed reactor. Coupling non- thermal plasma (NTP) with supported iron sulfide catalyst dramatically promotes SO_2 reduction at low temperatures, enhancing SO_2 conversion by 200% and 100% using H_2 and CH_4, respectively. Interestingly, under plasma condition, zinc sulfide catalyst showed high SO_2 hydrogenation activity, although it is thermally inactive even at high temperature. The possible origin of these synergetic effects and reaction mechanizes are proposed.

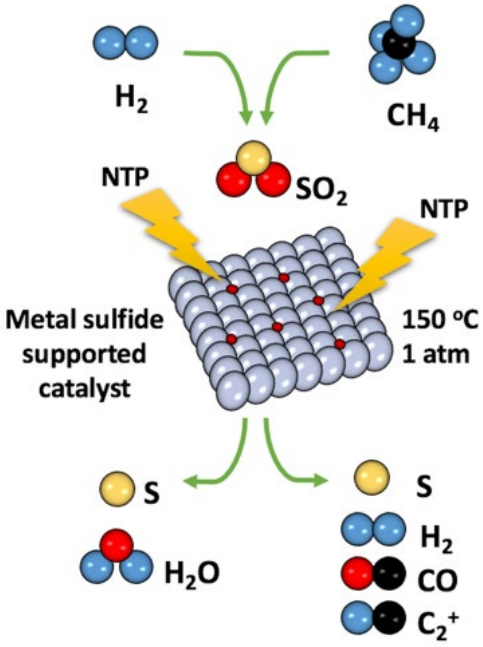

High Mobility and Drive Current ZnO Thin Film Transistors

Presenter: Sang H. Yoo (shy26.psu@gmail.com)
Advisor: Enrique D. Gomez (edg12@psu.edu) & Thomas N. Jackson (tnj1@psu.edu)

Thin film transistors (TFTs) are widely utilized in the display industry as select devices for pixel data and also have potential for 3D ICs and for flexible and large area electronic applications. Recently, oxide semiconductors such as indium gallium zinc oxide (IGZO) and zinc oxide (ZnO) have gained interest because they can provide improved mobility and stability compared to amorphous silicon and reduced manufacturing cost compared to polysilicon. ZnO TFTs with field-effect mobility > 100 cm^2/Vs have been demonstrated,[1] but these devices were fabricated using pulsed laser deposition (PLD), which may limit large-area and low-cost applications. In contrast to PLD, plasma-enhanced atomic layer deposition (PEALD) is an attractive deposition technique for high-volume manufacturing of oxide semiconductor devices and especially for ZnO. In this work, we have demonstrated a simple process modification using a N_2O plasma-based passivation layer that improves the performance of PEALD ZnO TFTs. ZnO TFTs with 5 µm channel lengths, PEALD ZnO active layer, and N_2O plasma based PEALD Al_2O_3 passivation layer exhibit drive currents >250 mA/mm and field-effect mobilities >80 cm^2/Vs. The devices were measured with low duty cycle pulsed measurements to minimize device heating effects and the resulting large drive current and high large signal mobility indicate that the results are not due to measurement artifacts. The high current and mobility of the N_2O PEALD passivated ZnO TFTs remained even when the passivation layer was completely etched off, suggesting that the high performance of the ZnO TFTS does not come from the passivation layer itself, but rather from modification of the ZnO active layer during the N_2O PEALD Al_2O_3 passivation process. The high performance of these devices is of interest for 3D ICs and other applications.

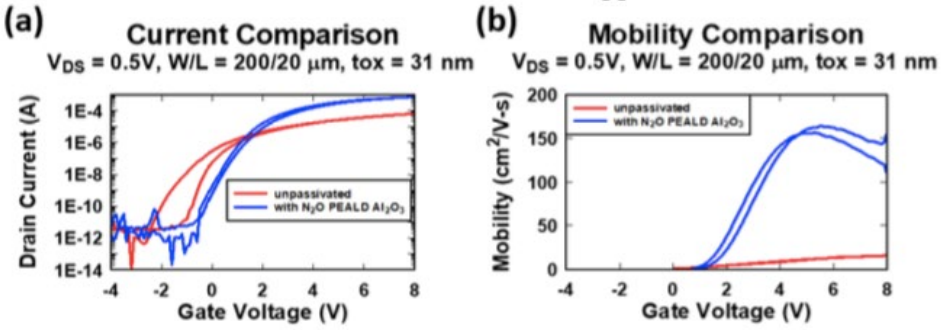

Figure 1. a) Linear region I_D versus V_{GS} for unpassivated and N_2O PEALD Al_2O_3 passivated ZnO TFTs; b) Linear region mobility for unpassivated and N_2O PEALD Al_2O_3 passivated ZnO TFTs.

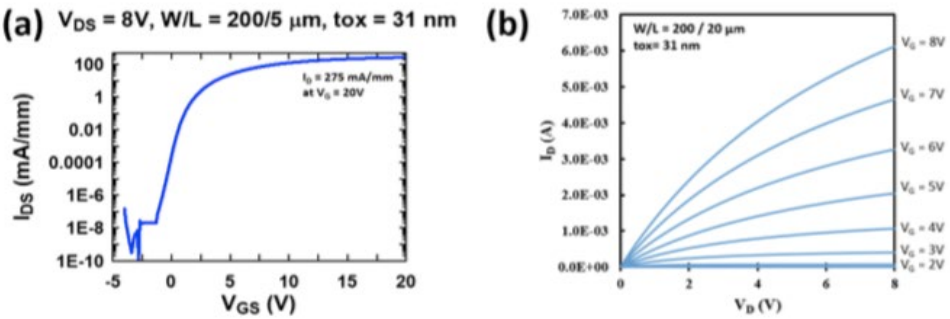

Figure 2. a) I_D versus V_{GS} for V_{DS} = 8V for N_2O PEALD Al_2O_3 passivated ZnO TFTs; b) I_D vs V_{DS} for N_2O PEALD Al_2O_3 passivated ZnO TFTs

1. B. Bayraktaroglu, et al., *IEEE Electron Device Lett.*, **29**, pp. 1024-1026 (2008).

Hydrothermal Valorization of Food Waste

Presenter: Bita Motavaf (bvm5395@psu.edu)
Advisor: Philip E. Savage (pes15@psu.edu)

A very large amount of food produced for human consumption, approximately 1.3 billion tons, is wasted globally per year.[1] Food waste has high moisture content with low energy density. A very common practice is disposing food waste in landfill, which consequently leads to decomposition of organic matter, emission of greenhouse gases and ground water contamination. Hydrothermal treatment, as a way to manage food waste, uses water as a reaction medium to convert wet biomass into energy dense biocrude by taking advantage of its properties at sub and super critical conditions. However, most other thermochemical processes require dry feed stock. We subjected a mixture of common consumed food items representing food waste to hydrothermal liquefaction (HTL). The intention of this work is reporting the details in yields and molecular composition of the products from a systematic study of HTL over a broad range of reaction conditions as water goes through phase change. Highest bio- crude yield of 35 wt. % has been observed at the saturated pressure for 350 °C among different range of pressures. For the same pressure of 35 MPa, the biocrude yield increased with temperature for subcritical temperature and dropped gradually after it passed the critical point. Water-soluble products, gases and solid residues were the additional products. The aqueous phase product yields were considerably high at lower temperatures and decreased as temperature increased. Gaseous products were highest at 500°C and 600 °C due to the hydrothermal gasification process. No loading effect has been observed on product yields. However, batch holding time seemed to be an affective factor. A drop of biocrude yield after 18 minutes suggested its decomposition after certain amount of time. Ultimately, we aim to analyze and characterize the products to reveal how products composition and higher heating values of biocrude changes with reaction conditions.

References: [1] Gustavsson, J. et al., 2013. The methodology of the FAO study: " Global Food Losses and Food Waste - extent, causes and prevention " -FAO, 2011 By SIK -The Swedish Institute for Food and Biotechnology.

High-Performance Multi-Component Organic Solar Cells

Presenter- Alperen Ayhan(iaa112@psu.edu)
Advisor – Dr.Enrique Gomez (edg12@psu.edu)

Multi-component Organic Solar Cells (MOSCs), consisting of multiple donor or acceptor materials in one photoactive layer, recently have emerged as one of the most promising strategy for broadening the light absorption spectrum and enhancing the power conversion efficiency (PCE) of photovoltaic devices compared with traditional binary solar cells. To enable efficient separation, transport and collection of charges, the photoactive layer morphology plays a dominating role for high-performance OSCs because there are some critical challenging issues such as controlling the phase separation and domain size of the device components. Furthermore, the chemical structure and the selection of compatible several components to form multi-mixture are one of the key factors on controlling morphology and PCE advancement in OSCs. In the chemical structures of OSCs components, side chains are mainly incorporated for the purpose of tuning the solubility of the molecule whereas backbone structure, consisting of conjugated functional groups, influences the electrical properties of the molecule. More importantly, their mutual influences determine molecular-scale structural information, such crystallinity, lattice constant, and orientation (lamellar and π-π stacking), which are beneficial to tune the morphology of the organic solar cells.

In this perspective, I propose that differentiating components from each other in the MOSCs by using advanced characterization techniques can lead to a better understanding on the phase behavior and improvement of the device performance. Here, I demonstrated high-efficiency OSCs by combining the organic semiconductor components complementing with each other, such as donors(D) (PffBT4T-2OD, PTB7-Th, PCDTBT, PM6) and acceptors(A) (PC70BM, IDIC, Eh-IDTBR, O-IDTBR, COi8FDIC, Y6), and their photovoltaic properties and morphology modulation were studied through optimizing processing parameters such as polymer concentration, D:A1:A2 ratio, thermal annealing, and adding additives. The effect of these parameters on the structural, morphological, electrical, and photovoltaic properties were systematically investigated by performing UV-Vis absorption, Grazing-Incidence Wide-Angle X-ray Scattering (GIWAXS), and Energy-Filtered Transmission Electron Microscopy (EFTEM). This work shows multicomponent systems composed of morphologically compatible donors and acceptors at their comparable loadings can achieve fibril-like nanostructure features resulting in improving phase separation, a remarkable high PCE, significant enhancement of short-circuit current due to broadening of the absorption spectrum, and the fill factor. We attribute that the high morphology compatibility of the multicomponent system can benefit to optimize electron/hole mobility and diminish recombination. This study reveals the correlation of the morphology characteristic with the device performance and offer new insight from the perspective of morphology modulation for constructing efficient MOSCs.

DFT analysis of Amino Acid functionalization of Hematite for electroreduction catalysis

Presenter: Sharad Maheshwari (sum458@psu.edu)
Advisor: Michael J. Janik (mjanik@psu.edu)

In a future with plentiful renewable electricity, electro-chemical systems to carry out chemical transformations can provide an efficient and sustainable alternative to fossil-fuel based energy consumption. Several important chemical reactions, such as CO_2 and N_2 reduction, have electro-chemical counterparts to form useful products through a series of proton-coupled electron transfer (PCET) reactions. The activity and selectivity of PCET reactions can significantly be impacted by the electrode-electrolyte interfacial properties, and tuning this near-surface environment can be used as a control towards developing active and selective electrochemical conversions. Surface-bound amino acid chains can be used to alter the electrocatalytic performance by altering the active site structure and local environment.

We first use a simple Density Functional Theory (DFT) based approach to estimate the electrochemical barriers [1] to elucidate the elementary kinetics of the possible associative mechanisms for N_2 electroreduction (NRR) on two low index surfaces of Fe [2]. Calculated activation barriers suggest significantly larger overpotentials for NRR than those inferred from consideration of only elementary reaction free energies. Key step barriers on low index surfaces of late transition metals resulted in a "kinetic volcano" for nitrogen reduction over (111) surfaces of FCC metals. This analysis suggests that transition metal catalysts will be ineffective for NRR, due to high elementary step barriers and low selectivity [3].

We further use DFT to study the surface binding of short amino acid chains on Fe_2O_3 surfaces to understand how they alter the interfacial environment through surface-ligand interactions. We examine the effects of small amino acid binding on the stability of different Fe_2O_3 terminations in the electrochemical environment. We consider how presence of continuum solvation affects the binding preferences of the amino acid. Coverage effects on binding energies are also evaluated.

Significance
This work demonstrates the extreme challenge in developing active and selective N_2 electroreduction catalyst to produce ammonia. Also, use of amino acid as co-catalyst to modify catalyst surface and environment provides a unique design variable to improve catalytic activity and selectivity.

1. G. Rostamikia et al., J. Power Sources 196(22), 9228–9237 (2011).
2. S. Maheshwari et al., J. Chem. Phys. 150, 041708 (2018)
3. G. Rostamikia et al., Cat. Sci. & Tech (In Press)

Morphing simulations reveal architecture effects on polymer miscibility in bead spring chains

Presenter: Shreya Shetty (sus498@psu.edu)
Advisor: Enrique Gomez (edg12@psu.edu) & Scott T. Milner (stm9@psu.edu)

The Flory Huggins interaction parameter χ quantifies the excess free energy of mixing two polymers and governs phase behavior in polymer blends and block copolymers. Chain architecture affects how chains pack in the melt, which can significantly influence χ. To explore this, we investigate χ for different architectures of flexible bead spring chains, using molecular dynamics simulations and our recently developed "morphing" method to compute the excess free energy of mixing. We examine blends in which both chain species have the "polypropylene" bead-spring structure, but one species has beads with a slightly weaker interaction (Figure 1) – either the side beads (case 1), main chain beads (case 2), or branch point beads (case 3). We use our method to find χ for all three cases, for which random mixing models would give identical results. We observe that strongest repulsion is experienced in the case of side bead, as a result of higher accessibility to differently interacting bead. Finally, we compare our values with predictions from PRISM, with correlation functions from simulations as input, as a purely simulation-based test of PRISM. We observe that the PRISM predictions for χ, despite being of the same order as simulation predictions, are negative for certain cases and is highly sensitive to initial guess used to solve PRISM equations.

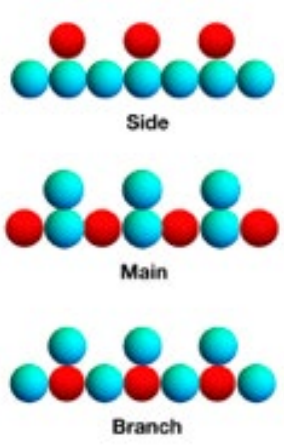

Figure 1. Different architectures explored in the morphing simulations

Metal-Organic Framework (MOF) assisted Li^+ conduction in solid polymer electrolyte for application in lithium-ion batteries

Presenter: Nagma Zerin (nzz5@psu.edu)
Advisor: Janna Maranas (jmaranas@psu.edu)

Solid polymer electrolytes (SPEs) are safer and more efficient alternatives to the current organic liquid electrolytes (toxic and flammable) used in lithium-ion batteries. The most important advantage is that SPEs can be used with lithium metal as the anode. The theoretical capacity of lithium metal anode is about 10 times higher than the present graphite anode, which is directly proportional to the number of miles that can be driven per charge by an electric car. Liquid electrolytes are incompatible with Li metal anode because of dendrite formation on lithium metal surface during battery charging.

The most common SPE is semi-crystalline polymer poly(ethylene oxide) (PEO) dissolving a lithium salt (e.g., $LiClO_4$). PEO is popular due to its ability to dissolve alkali metal salts easily, and commercial availability at a reasonable cost. However, the PEO based electrolytes have poor ionic conductivity, which does not meet the performance demands for practical battery applications. It is believed that ion conduction in PEO based electrolytes depends on polymer mobility in amorphous domains, where lithium ions travel by coordinating with the ether oxygens of the PEO chain. Thus, to increase polymer mobility associated conductivity, a considerable amount of research is focused on lowering the glass transition temperature of SPEs. However, this approach compromises the polymer stiffness, which makes the SPE incompatible to be used with lithium metal as the anode. Crystalline SPEs are promising alternatives to dissociate conductivity from polymer mobility and improve polymer stiffness. The focus of our research is to improve lithium-ion conduction in crystalline SPEs and to achieve that we are incorporating 2D Cu-based metal-organic framework (MOF) as the nanofiller.

Probing Nanocrystal Shape Transformations Using Replica-exchange Molecular Dynamics

Presenter: Tianyu Yan (tuy15@psu.edu)
Advisor: Kristen Fichthorn (kaf2@psu.edu)

Solution-phase syntheses have produced an astounding variety of metal nanocrystal shapes with unique properties that depend on shape. Studies have shown that nanocrystal shapes often depend on the shape of the "seeds" – crystallites in the 1-10 nm size range that form subsequent to nucleation. The shapes of seeds (single crystal and twinned) are highly fluxional and sensitive to the solution environment surrounding them. Though many studies have probed minimum-energy shapes for small clusters in vacuum, very few studies have probed the effect of temperature and solution environment.

Focusing on Ag nanoclusters described by an embedded-atom method potential, we use replica-exchange molecular dynamics (REMD) simulations to generate ensembles of equilibrium shapes for Ag nanoclusters in the 2-10 nm size range as a function of temperature.

We apply Common Neighbor Analysis (CAN) to identify the crystallographic environments of cluster atoms and we create barcodes to characterize cluster structures. These studies show that clusters fall within a few structural motifs that can change with temperature in vacuum. We find the distribution of nanocrystal shapes changes sensitively with nanocrystal size, even for size changes of a few atoms. We find that preferred shapes occur at various "magic sizes". Small Ag nanocrystals melt significantly below its bulk melting point.

In the future, we will study how the cluster interfacial free energies and the energetically favored shapes can be altered in a solution environment by means of REMD simulations.

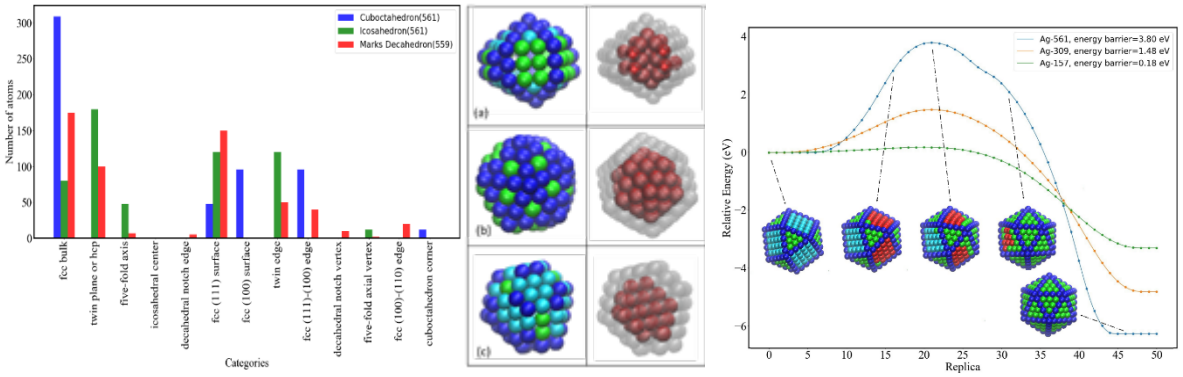

Morphology and transport properties of ion-exchange membranes for applications in advanced flow batteries

Presenter: Nayan Saikia (njs30@psu.edu**)**
Adviser: Dr. Michael Hickner (mah49@psu.edu)

Ion exchange membranes (IEMs) are electrically conductive polymers that are responsible for selectively transporting ions. There are broadly two different types of IEMs: cation or proton exchange membrane (PEM) which selectively transporting cations and anion exchange membrane (AEMs) which transport anions. Irrespective of the type they find applications in a variety of technologies such as advance batteries, fuel cells and electrodialysis. Recently, a lot of emphasis has been made in evaluating these membranes for desirable properties such as high conductivity (> 10 mS cm-1), low permeability (<10-9 cm2/s) and stability in acidic and basic conditions for greater than 1000 hours. We aim to take forward this understanding of membrane transport properties and link it to the morphology of these polymers. Different morphologies arise because ionic polymers are made up of a hydrophobic backbone and hydrophilic side chain, which are incompatible to each other and causes the membrane to phase separate. Ordered phase separation can give rise to channels (Nafion) and ionic highways which boosts the conductivity significantly1. We employ energy filtered transmission electron microscopy (EFTEM) and energy dispersive spectroscopy (EDS) to image ionic domains and generate elemental maps which can help us in understanding the fundamental link between morphology and physical properties of the membrane.

Reference

1. Pan, J.; Chen, C.; Li, Y.; Wang, L.; Tan, L.; Li, G.; Tang, X.; Xiao, L.; Lu, J.; Zhuang, L. Energy Environ. Sci. 2014.

POSTER SESSION ABSTRACTS

Effect of interfacial electric fields on elementary catalytic kinetics on transition metal surfaces

Presenter: Naveen Agarwal (nua155@psu.edu)
Advisor: Michael J. Janik (mjanik@psu.edu)

Electric fields over 0.1 V/Å alter the energies of molecular orbitals of adsorbates, they can also change the activation barriers for reactions and hence their associated kinetic parameters, making electric fields relevant to the field of catalysis[1]. In an electrochemical cell, a potential drop of 1.2 V across the interfacial layer of the order of 3-8 Angstrom can generate an electric field of order 0.5 V/Å. We are applying an external field using VASP in metal-vacuum interface simulation to investigate the relative sensitivity for the energetics of elementary bond cleavages (C-H, N-H, and O-H), which are relevant to a broad range of electrochemical transformations such as CO_2 reduction to hydrocarbons, water oxidation or H_2-O_2 fuel cell and nitrogen reduction to ammonia. Our broader goal is to utilize DFT with an applied electric field to determine how electric field differentially promote/hinder specific bond formation or cleavages across a variety of transition metal surfaces. Our preliminary results show that the presence of a shuttling agent such as H_2O facilitating for a Heyrovsky O-H cleavage is affected significantly differently by an applied electric field in comparison to Tafel C-H cleavage. Interestingly, the trends of such contrast also have been shown to depend on the nature of metal surface and the polarity of bond cleavage. We plan to extend these studies to guide design principles for electrocatalytic reactions which are affected by the presence of interfacial electric fields.

References:

1. Che, F.; Gray, J. T.; Ha, S.; Kruse, N.; Scott, S. L.; McEwen, J.-S., Elucidating the Roles of Electric Fields in Catalysis: A Perspective. *ACS Catalysis* **2018,** *8* (6), 5153-5174.

Understanding the growth mechanism of five-fold twinned copper nanowire using atomic-scale simulations and the application of machine learning techniques on silver nanoclusters

Presenter: Saksham Phul (sup864@psu.edu)
Advisor: Kristen Fichthorn (kaf2@psu.edu)

As the demand for touch screen devices increases, there is a need for a better and cost-effective material which is highly transparent and conductive. Nanowire finds their application in transparent conducting electrodes having high conductivity and transmittance. Copper nanowires may serve as a low-cost alternative to Indium tin oxide (ITO) and silver nanowire in thin-film solar cells, touch screens, and flexible displays. We examine the anisotropic growth mechanism of a copper nanowire in vacuum. We incorporate atomic scale methods to examine the intrinsic shape and size of the seed. The seed is similar to a Marks decahedron with {111} notches to support growth and {110} steps to make the crystal thermodynamically more stable. Hopping barriers on {111} and {100} predict the preferential aggregation of atoms and relieve that seed would grow in diameter, not evolve into the nanowire in vacuum. We investigate the energetic preference for seeds with different diameters to grow into nanowires and find that beyond a diameter of 17-25 nm, there is an increasing thermodynamic driving force for nanowire growth. We find a heterogenous strain distribution leading to a variety of hopping barriers on both {100} and {111} facets and generating atom aggregation sites.

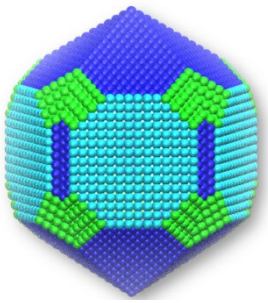

Figure 1: Estimated nanoseed of five-fold twinned copper nanowire from annealing MD simulations

The shape of a nanoseed is of prime importance as it plays a significant role in the morphology of an evolved nanowire. In this study, machine learning techniques were implemented to 127 atoms silver nanoseed to separate the possible number of clusters attained from 25 replica exchange molecular dynamics simulation. Unsupervised clustering techniques such as PCA, K means, Hierarchical Clustering was implemented on 25 shapes to segregate shapes into different clusters. Hierarchical Clustering algorithm has the best performance, dividing the ensemble of 25 shapes into 3 groups. The features correlation plot shows important connections among generated features.

Regulation of Histone Modifications via Matrix Stiffness during TGFβ1-induced Epithelial-Mesenchymal Transition

Presenter: Chinmay S. Sankhe (css313@psu.edu)
Advisor: Esther Gomez (ewg10@psu.edu)

Epithelial-Mesenchymal Transition (EMT) is a physiological process that is essential during embryogenesis and wound healing and is also a contributor to fibrosis and metastatic cancer[1]. EMT is promoted by increased stiffness that accompanies tumor progression and is characterized by loss of epithelial markers such as E-cadherin and gain of mesenchymal traits such as increased expression of cytoskeletal proteins and enhanced cell motility[3]. Furthermore, epigenetic reprogramming, including histone modifications, change chromatin structure and regulate gene transcription during EMT[2]; however, there is limited knowledge available on how mechanical signals control epigenetic remodeling of histones and subsequent transcriptional activation during EMT. Here, we synthesized hydrogels with mechanical properties that span that of normal and diseased mammary tissue and examined the response of mammary epithelial cells to transforming growth factor (TGF)β1-induced EMT. We found that matrix stiffness and TGFβ1 together enhanced the levels of the histone H3 lysine 36 methylation marker H3K36Me3, which is associated with active gene transcription. In addition, the levels of the histone H3 lysine 9 methylation marker H3K9Me3, associated with epithelial gene silencing, were enhanced by increasing matrix stiffness following TGFβ1 treatment. These observations suggest a regulatory role of matrix rigidity in the initiation and modulation of EMT through control of epigenetic reprogramming and gene transcription.

Combining X-Ray Spectroscopy and Scattering to Understand Cellulose Organization in Primary Plant Cell Walls

Presenter: Sintu Rongpipi (sxr95@psu.edu)
Advisor: Enrique D. Gomez (edg12@psu.edu) & Esther W. Gomez (ewg10@psu.edu)

Cellulose microfibrils are structural units found in primary cell walls of plants and their spatial arrangement strongly impacts cell wall mechanics and growth. While the mesoscale arrangement of cellulose microfibrils has been extensively studied by microscopy techniques, it remains a challenge to quantitatively extract characteristic length scales and resolve subtle changes in microstructure. Scattering methods provide a complementary approach to microscopy that can meet these needs; however, the cell wall is a heterogeneous mixture of several polysaccharides that have similar electron densities. As a result, conventional hard X-ray scattering cannot generate enough contrast to resolve the different elements of the polysaccharide network. Resonant soft X-ray Scattering (RSoXS) combines soft X-ray spectroscopy and scattering to provide elemental and chemical environment sensitivity which enables differentiation between the cell wall polysaccharides based on differences in composition.

We used RSoXS to extract average interfibrillar spacing between cellulose microfibrils. In the cell walls, calcium ions are localized to homogalacturonan in the pectin matrix in which the cellulose microfibrils are embedded. By tuning X-ray energy to the calcium L-edge, contrast between cellulose and pectin could be enhanced. Consequently, RSoXS profiles reveal an average center-to-center distance between cellulose microfibrils or microfibril bundles in primary cell walls. RSoXS investigations of primary cell walls of *Arabidopsis thaliana* reveal a change in cellulose microfibril organization with developmental age of tissue and investigations of cell wall mutants suggest a change in cellulose organization in the mutants. These findings provide important insights into the structure-functional relationship of cell walls that aid plant growth and development.